SUPPLEMENTAL MATERIAL

Klein et al., http://www.jem.org/cgi/content/full/jem.20150556/DC1

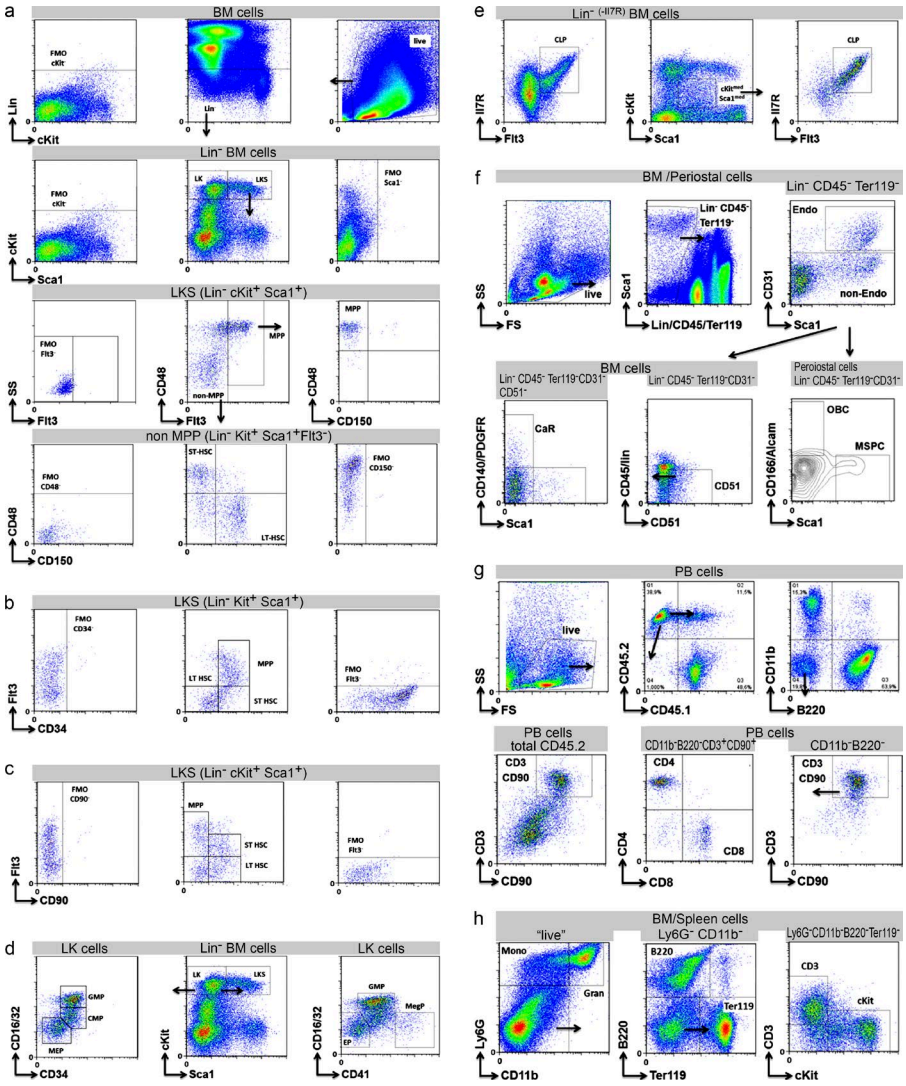

Figure S1. **Gating strategies for PB, spleen/BM cells analysis, and niche cell purification.** (a) Living BM cells (live) were separated from debris and all differentiated BM cells were depleted in order to get undifferentiated (Lin^-) BM cells (first row). The threshold could be defined using the fluorescence minus one (FMO) $cKit^-$ staining. Lin^- BM cells were further subdivided in Lin^-cKit^+ (LK) cells and $Lin^-cKit^+Sca^+$ (LKS) cells using the FMOs of $cKit^-$ and $Sca1^-$ (second row). LKS cells were subdivided in $Flt3^+$ multipotent progenitors (MPPs) and $Flt3^-$ short- and long-term HSCs (ST-HSCs, LT-HSCs, and non-MPP). To determine $Flt3^+$ MPPs, FMO $Flt3^-$ was used. Non-MPPs were further subdivided into $CD150^-CD48^+$ ST-HSCs and $CD150^+CD48^-$ LT-HSCs (fourth row). (b) LKS cells can also be partitioned into $CD34^-Flt3^-$ LT-HSCs, $CD34^+Flt3^-$ ST-HSCs, and $CD34^+Flt3^+$ MPPs. Gates adjusted by FMO performance. (c) LKS cells can also be partitioned into $CD90^+Flt3^-$ LT-HSCs, $CD90^+Flt3^{med}$ ST-HSCs and $CD90^-Flt3^+$ MPPs. Gates adjusted by FMO performance. (d) LK cells (center) were split into $CD34^+CD16/32^{high}$ granulocyte-macrophage progenitor (GMP), $CD34^+CD16/32^{med}$ common myeloid progenitor (CMP), and $CD34^-CD16/32^-$ megakaryocyte-erythroid progenitor (MEP) cells (left). LK cells (center) could also be subdivided into $CD41^+CD16/32^-$ megakaryocyte progenitor (MegP), $CD41^{med}CD16/32^+$ granulocyte-macrophage progenitor (GMP) and $CD41^-CD16/32^-$ erythroid progenitor (EP) cells (right). (e) Within the $Lin^{-(-Il7R)}cKit^{med}Sca1^{med}$ cells (center), $Flt3^+Il7R^+$ CLPs can be detected (right). If all $Lin^{-(-Il7R)}$ cells were used for analysis (left), the fraction of CLPs is degraded. (f) Gating strategy for niche cell isolation. $Lin^-CD45^-Ter119^-$ cells were gated and separated into endothelial Cells (Endo, $Lin^-CD45^-Ter119^-CD31^+Sca1^+$), expressing CD31/Sca1 and nonendothelial cells (non-Endo, $Lin^-CD45^-Ter119^-CD31^-$). Non-Endo bone-derived cells could be further subdivided into osteoblastic cells (OBCs; $Lin^-CD45^-Ter119^-CD31^-Sca1^-CD166^+$) and MSPCs (MSPC $Lin^-CD45^-Ter119^-CD31^-Sca1^+CD166^-$). Within Non-Endo BM-derived $CD51^+$ cells, Cxcl12-abundant reticular cells (CaR, $Lin^-CD45^-Ter119^-CD31^-CD51^+Sca1^-CD140^+$) were purified. (g) Gating strategy for PB cell analysis. In transplantation settings using CD45.1 and CD45.2 chimeric mice, CD45 discrimination was used to distinguish between host ($CD45.1^+$ or $CD45.2^+$), donor ($CD45.1^+$ or $CD45.2^+$), or recipient ($CD45.1^+CD45.2^+$). PB cells were split up into $CD11b^+$ myeloid cells, $B220^+$ B cells, and $CD11b^-B220^-$ cells which were $CD3^+CD90^+$ T cells. These cells were subdivided into $CD4^+$ T helper and $CD8^+$ T cytotoxic cells. (h) Gating strategy for BM and spleen cells. Cells were split up into $Ly6G^+CD11b^+$ granulocytes (Gran) and $Ly6G^-CD11b^+$ monocytes (Mono). $Ly6G^-CD11b^-$ cells could be subdivided into $Ter119^+$ erythroid cells or $B220^+$ B cells. $Ly6G^-CD11b^-Ter119^-B220^-$ were $CD3^+$ T cells or $cKit^+$ progenitor/stem cells. $CD3^+$ T cells could be further discriminated as already shown in g.

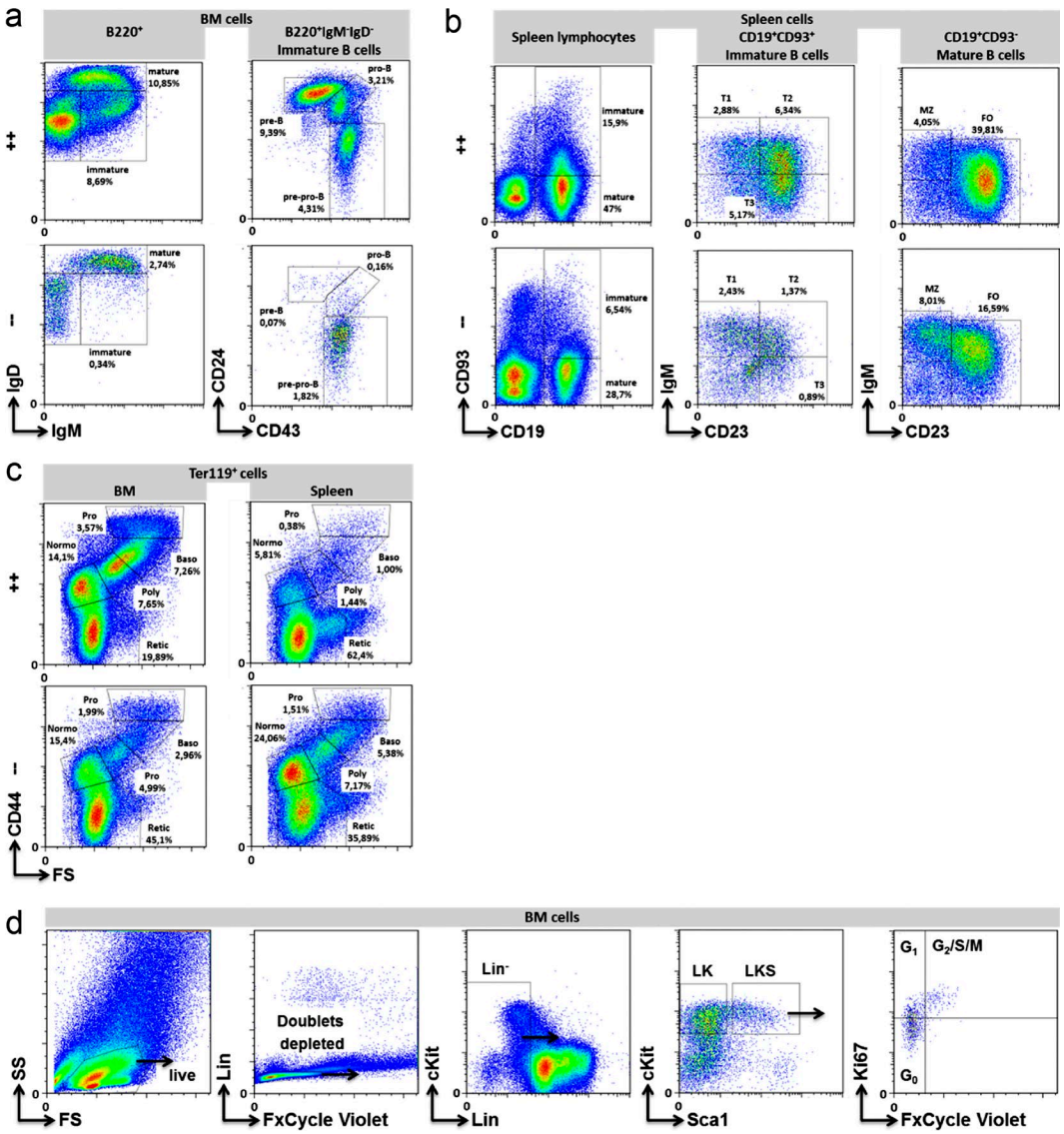

Figure S2. **Flow cytometry analyses.** (a) Flow cytometry analysis for B cell lymphopoiesis within the BM of WT and Ptch2$^{-/-}$ mice after 12 mo. B220^{+} BM cells were subdivided into mature (B220^{+}IgM$^{+/-}$IgD^{+}), immature (B220^{+}IgM^{+}IgD^{-}), prepro–B cells (B220^{+}IgM^{-}IgD^{-}CD43^{+}CD24^{-}), pro–B cells (B220^{+}IgM^{-}IgD^{-}CD43^{+}CD24^{+}), and pre–B cells (B220^{+}IgM^{-}IgD^{-}CD43^{-}CD24^{+}). One representative example is shown for each genotype. (b) Flow cytometry analysis for B cell maturation within the spleen of WT and Ptch2$^{-/-}$ mice after 12 mo. Spleen cells were subdivided into mature (CD19^{+}CD93^{-}) and immature (CD19^{+}CD93^{+}) populations. Mature B cells were subdivided into marginal zone (MZ) B cells (CD19^{+}CD93^{-}CD23^{-}IgM^{+}) and follicular (FO) B cells (CD19^{+}CD93^{-}CD23^{+}IgM$^{-/+}$). Immature B cells were subdivided into transitional (T) B cells T1 (CD19^{+}CD93^{+}CD23^{-}IgM^{+}), T2 (CD19^{+}CD93^{+}CD23^{+}IgM^{+}), and T3 (CD19^{+}CD93^{+}CD23^{+}IgM^{-}) cells. One representative example is shown for each genotype. (c) Flow cytometry analysis of BM and spleen cells for erythroid progenitors of WT and Ptch2$^{-/-}$ mice after 12 months. Ter119^{+} cells could be subdivided into all stages of erythropoiesis: FS^{high}CD44^{high} proerythroblasts (Pro), FS^{high}CD44^{med} basophilic eryhtroblasts (Baso), FS^{med}CD44^{med} polychromatic erythroblasts (Poly), FS^{low}CD44^{med} normoblasts, and FS^{low}CD44^{low} reticulocytes (Retic). One representative example is shown for each genotype. (d) Gating strategy for LKS cell cycle analysis (BM cells). HSCs are subdivided into Ki67^{-}FxCycleViolet^{low} cells (G_0), Ki67^{+} FxCycleViolet^{low} cells (G_1), and Ki67^{+} FxCycleViolet^{high} cells (G_2/S/M).

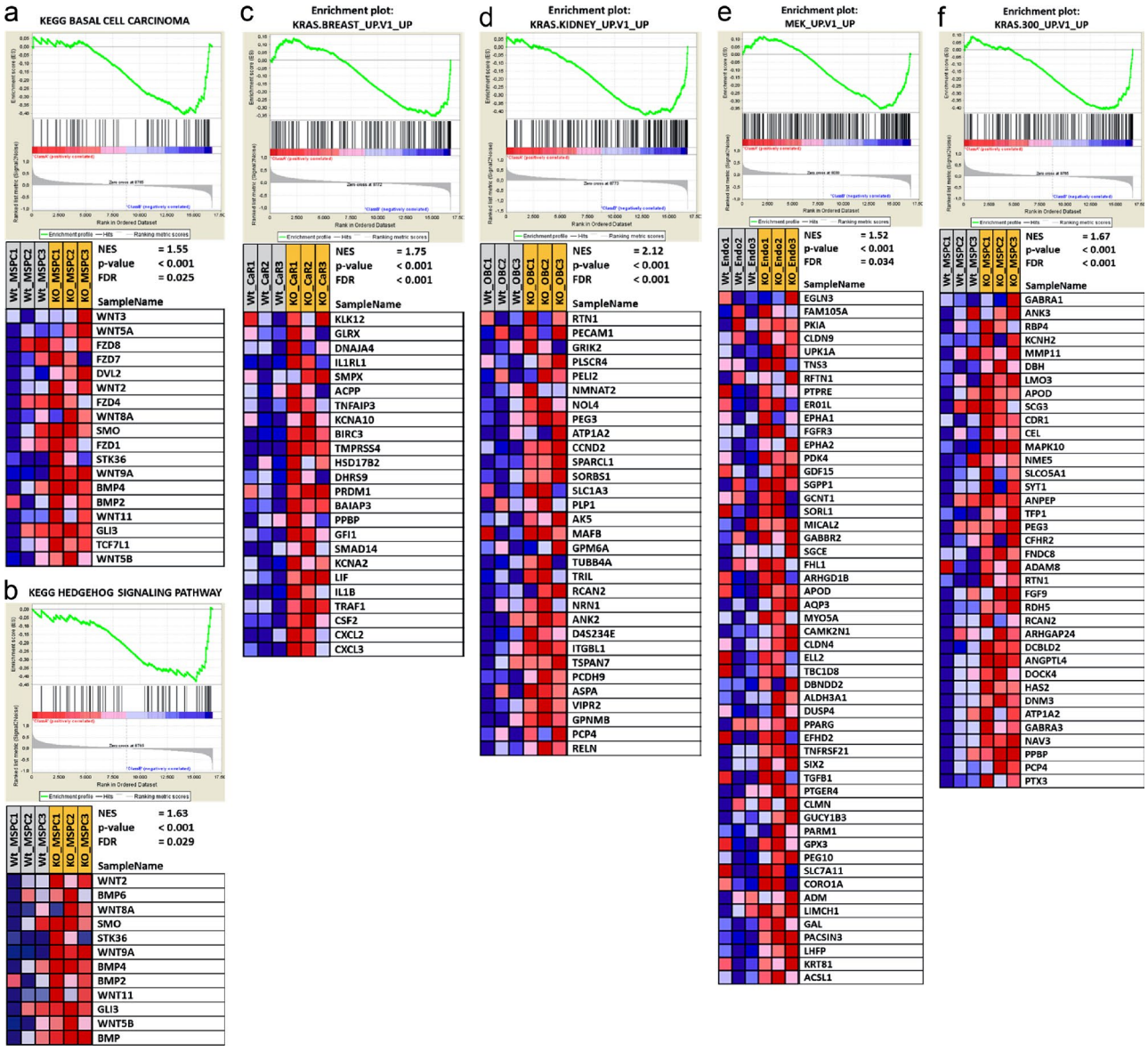

Figure S3. **Enrichment plots and heat maps for core enrichment genes.** (a and b) Enrichment plots and heat maps for core enrichment genes were generated by GSEA using the KEGG gene sets. NES, nominal p-value, and FDR are shown for each gene set. Comparison of WT versus Ptch2$^{-/-}$ MSPCs identifies up-regulation of the Basal cell carcinoma. (a) Gene set and up-regulation of the Hedgehog signaling pathway. (b) Gene set. (c–f) Enrichment plots and heat maps for core enrichment genes were generated by GSEA using the oncogenic signature gene sets. NES, nominal p-value, and FDR are shown for each gene set. Comparison of WT versus Ptch2$^{-/-}$ CaR (c), OBCs (d), endothelial cells (e) and MSPCs (f) reveals an increase of Map–Erk kinase signaling within all four Ptch2$^{-/-}$ subpopulations.

Table S1. **Patient characteristics**

ID	Sex	Age	Material	Diagnosis	Genetic aberration
1	F	-	EDTA-PB	Control	n.d.
2	M	-	EDTA-PB	Control	n.d.
3	F	-	EDTA-PB	Control	n.d.
4	M	-	EDTA-PB	Control	n.d.
5	M	-	EDTA-PB	Control	n.d.
6	M	-	EDTA-PB	Control	n.d.
7	M	-	EDTA-PB	Control	n.d.
8	F	-	EDTA-PB	Control	n.d.
9	M	-	EDTA-PB	Control	n.d.
10	F	52	EDTA-PB	polycythemia vera	Jak2V617F
11	F	63	EDTA-PB	polycythemia vera	Jak2V617F
12	F	71	EDTA-PB	polycythemia vera	Jak2V617F
13	F	63	EDTA-PB	polycythemia vera	Jak2V617F
14	M	44	EDTA-PB	polycythemia vera	Jak2V617F
15	M	48	EDTA-PB	polycythemia vera	Jak2V617F
16	F	45	EDTA-PB	polycythemia vera	Jak2V617F
17	F	52	EDTA-PB	polycythemia vera	Jak2V617F
18	F	58	EDTA-PB	polycythemia vera	Jak2V617F
19	M	49	EDTA-PB	polycythemia vera	Jak2V617F
20	M	63	EDTA-PB	polycythemia vera	Jak2V617F
21	M	23	EDTA-PB	polycythemia vera	Jak2V617F
22	M	62	EDTA-PB	polycythemia vera	Jak2V617F
23	M	65	EDTA-PB	OMF	Jak2V617F
24	M	71	EDTA-PB	OMF	Jak2V617F
25	F	66	EDTA-PB	OMF	Jak2V617F
26	M	53	EDTA-PB	OMF	Jak2V617F
27	F	49	EDTA-PB	CML, BC	BcrAbl
28	M	55	EDTA-PB	CML, BC	BcrAbl
29	M	37	EDTA-PB	CML, BC	BcrAbl
30	F	78	EDTA-PB	CML, BC	BcrAbl
31	M	46	EDTA-PB	CML, CP	BcrAbl
32	F	57	EDTA-PB	CML, CP	BcrAbl
33	M	18	EDTA-PB	CML, CP	BcrAbl
34	M	84	EDTA-PB	CML, CP	BcrAbl
35	F	63	EDTA-PB	CML, CP	BcrAbl
36	M	43	EDTA-PB	CML, CP	BcrAbl
37	M	53	EDTA-PB	CML, CP	BcrAbl
38	M	35	EDTA-PB	CML, CP	BcrAbl
39	F	44	EDTA-PB	CML, CP	BcrAbl
40	M	61	EDTA-PB	sec. AML	SF3B1, RUNX1
41	M	61	EDTA-PB	sec. AML	KIT D816V
42	F	78	EDTA-PB	sec. AML	complex karyotype
43	M	70	EDTA-PB	sec. AML	47XY +8 [1]+
44	M	75	EDTA-PB	sec. AML	complex karyotype
45	M	53	EDTA-PB	sec. AML	complex karyotype
46	F	50	EDTA-PB	sec. AML	IDH2
47	M	55	EDTA-PB	sec. AML	del12q
48	M	74	EDTA-PB	sec. AML	$FLT3^+$
49	M	73	EDTA-PB	AML	$FLT3^-$, NPM1
50	M	74	EDTA-PB	AML	$FLT3^-$
51	M	54	EDTA-PB	AML	$FLT3^-$
52	M	33	EDTA-PB	AML	$FLT3^-$
53	F	51	EDTA-PB	AML	$FLT3^-$, NPM1
54	M	36	EDTA-PB	AML	$FLT3^+$, del16q22(CBFβ)
55	F	55	EDTA-PB	AML	$FLT3^-$, NPM1
56	F	64	EDTA-PB	AML	$FLT3^-$, NPM1
57	F	55	EDTA-PB	AML	$FLT3^-$, NPM1
58	M	73	EDTA-PB	AML	$FLT3^+$
59	M	49	EDTA-PB	AML	$FLT3^+$
60	M	67	EDTA-PB	AML	n.d.
61	M	63	EDTA-PB	AML	$FLT3^+$
62	M	48	EDTA-PB	AML	$FLT3^+$

Table S1. **Patient characteristics** *(Continued)*

ID	Sex	Age	Material	Diagnosis	Genetic aberration
63	F	78	EDTA-PB	AML	$FLT3^+$
64	F	47	EDTA-PB	AML	45,XX,-7
65	M	65	EDTA-PB	AML	$FLT3^+$
66	F	60	EDTA-PB	AML	karyotype 47 XX
67	F	74	EDTA-PB	AML	48-49,XX, + r(8)x2-3
68	F	76	EDTA-PB	AML	$FLT3^+$

Characteristics from healthy controls and patients (M, male; F, female), whose PB was used for mRNA extraction and purification and RT-PCR analysis. n.d., not detected; OMF, osteomyelofibrosis; BC, blast crisis; CP, chronic phase.

Table S2. **Molecular Signature Database oncogenic signatures**

Gene sets/pathways	CaR NES	OBC NES	MSPC NES	Endo NES
KRAS.300 UP.V1 UP		−1,600	−1,670	−1,530
KRAS.50 UP.V1 UP	−1,200	−1,240	−1,500	−1,560
KRAS.600 UP.V1 DN		−1,520		
KRAS.600 UP.V1 UP		−1,650	−1,380	−1,260
KRAS.600.LUNG.BREAST UP.V1 DN		−1,510		
KRAS.600.LUNG.BREAST UP.V1 UP	−1,280	−1,540	−1,440	
KRAS.AMP.LUNG UP.V1 DN			−1,340	
KRAS.AMP.LUNG UP.V1 UP	−1,390	−1,310	−1,340	−1,580
KRAS.BREAST UP.V1 UP	−1,750	−1,590		
KRAS.BREAST UP.V1 UP		−1,650		
KRAS.KIDNEY UP.V1 DN		−1,450		
KRAS.KIDNEY UP.V1 UP		−2,120	−1,950	
KRAS.LUNG UP.V1 UP				−1,420
KRAS.LUNG.BREAST UP.V1 DN		−1,840	−1,240	
KRAS.LUNG.BREAST UP.V1 UP	−1,730	−2,020	−1,310	
KRAS.PROSTATE UP.V1 DN			−1,310	
MEK UP.V1 UP		−1,220		−1,520

Molecular Signature Database subcollection "oncogenic signatures" was used to identify dysregulated Map–Erk pathway members. WT or $Ptch2^{-/-}$ niche cell subpopulations were analyzed and compared to each other. Negative results represent up-regulation in $Ptch2^{-/-}$ cells. Settings: NES <−1.20 (meaning 20% up-regulated in $Ptch2^{-/-}$), nominal p-value < 0.001, and FDR < 0.25.

Table S3. **Genes and primers**

Gene locus	Species	Primer	Vendor
TaqMan Primer, human			
BCL2	Hs	00608023_m1	Life Technologies
CCND1	Hs	00765553_m1	Life Technologies
DHH	Hs	00928824_m1	Life Technologies
GAPDH	Hs	02758991_g1	Life Technologies
GLI1	Hs	00171790_m1	Life Technologies
PTCH1	Hs	00970980_m1	Life Technologies
PTCH2	Hs	01085643_m1	Life Technologies
SHH	Hs	00179843_m1	Life Technologies
SMO	Hs	01090242_m1	Life Technologies
TaqMan Primer, mouse			
Angpt1	Mm	00456503_m1	Life Technologies
Bcl2	Mm	00477631_m1	Life Technologies
Ccnd2	Mm	00438071_m1	Life Technologies
Cxcl12	Mm	00445553_m1	Life Technologies
Dhh	Mm	030535542_s1	Life Technologies
Gapdh	Mm	4352339E	Life Technologies
Gli1	Mm	00494645_m1	Life Technologies
Ihh	Mm	00439613_m1	Life Technologies
Jag1	Mm	00496902_m1	Life Technologies
KitL	Mm	00442972_m1	Life Technologies
Ptch1	Mm	01306904_m1	Life Technologies
Ptch2	Mm	00436047_m1	Life Technologies
Shh	Mm	00436527_m1	Life Technologies
Smo	Mm	01162710_m1	Life Technologies
Spp1	Mm	00436767_m1	Life Technologies
Thpo	Mm	00437040_m1	Life Technologies
Tnfsf11	Mm	00441906_m1	Life Technologies